Alone in a crowd: Effect of a nonfunctional lateral line on expression of the social hormone *parathyroid hormone 2*.

Alexandra Venuto[1], Cameron P. Smith[1,2], Marybelle Cameron-Pack[3], and Timothy Erickson[3]

1. East Carolina University, Greenville, NC, USA
2. East Carolina University School of Dental Medicine, Greenville, NC, USA
3. University of New Brunswick, Fredericton, NB, CAN

Corresponding author: Timothy Erickson, timothy.erickson@unb.ca

Key words: hair cells, lateral line, neuropeptide, parathyroid hormone, social brain, zebrafish

SUMMARY STATEMENT

Expression of the pro-social neuropeptide *pth2* is downregulated in larval zebrafish with a congenital loss of lateral line function. Thus, even in social environments, fish with compromised lateral lines may experience chronic loneliness.

ABSTRACT

Parathyroid hormone 2 (Pth2) is a vertebrate-specific neuropeptide whose thalamic expression is upregulated by social contact with conspecifics. However, social interactions fail to stimulate *pth2* expression in isolated zebrafish whose lateral line hair cells have been chemically ablated. These results suggest that modulation of *pth2* by social context is acutely dependent on mechanosensory information from the lateral line. However, it is unclear how a congenital loss of lateral line function influences the ability of zebrafish to interpret their social environment. In this study, we measure *pth2* levels in zebrafish mutants lacking hair cell function in either the lateral line only, or in both the inner ear and lateral line. Socially-raised lateral line mutants express lower levels of *pth2* relative to wild type siblings, but there is no further reduction when all sensory hair cells are nonfunctional. However, social isolation of hair cell mutants causes a further reduction in *pth2* expression, pointing to additional unidentified sensory cues that influence *pth2* production. Lastly, we report that social context modulates fluorescent transgenes driven by the *pth2* promoter. Altogether, these data suggest that lateral line mutants experience a chronic sense of isolation, even when raised in a social environment.

INTRODUCTION

The complex relationship between the brain and social behavior has been studied across animal species for decades (Brothers, 1990; Chen and Hong, 2018; Kravitz and Huber, 2003; Robinson et al., 2008). Different social contexts can evoke a wide range of emotions, from joy and positivity (Burgdorf and Panksepp, 2006; Panksepp and Burgdorf, 2003) to fear and aggression (Amaral, 2002; Neumann et al., 2010) with a high level of plasticity (Chen and Hong, 2018; Kolb and Whishaw, 2003). In situations of social isolation, many animals exhibit anxious behaviors in addition to neurochemical changes in the brain (Amaral, 2002; Mumtaz et al., 2018; Shams et al., 2017; Weiss et al., 2004).

Previous studies have shown that social behavior is modulated by a suite of neuropeptides (Oldfield and Hofmann, 2011; Panksepp et al., 2007; Wu et al., 2003). Parathyroid hormone 2 (Pth2, (formerly known as tuberoinfundibular peptide of 39 residues or TIP39) is a neuropeptide expressed in the vertebrate thalamus, which is a sensory integration and relay center (Anneser et al., 2020; Bhattacharya et al., 2011; Dobolyi et al., 2012). In rodents, the PTH2 receptor is expressed in several nuclei throughout the central nervous system (Dobolyi et al., 2012). Zebrafish have two *pth2r* paralogs, *pth2ra* and *pth2rb,* each with distinct expression patterns in the fish brain (Seitz, 2019). Activation of PTH2R increases intracellular cAMP levels and can modulate neuroendocrine activity in the hypothalamic–pituitary–adrenal (HPA) axis (Dimitrov and Usdin, 2010). PTH2-PTH2R signaling influences several behaviors, including maternal care (Cservenák et al., 2013), pain sensitivity (Dimitrov et al., 2010; Dimitrov et al., 2013; LaBuda and Usdin, 2004), and anxiety-like responses (Anneser et al., 2022; Coutellier and Usdin, 2011; LaBuda et al., 2004).

Recent work suggests that Pth2 signaling promotes social interactions between conspecifics. In zebrafish, *pth2* mutants exhibit decreased preference for conspecifics (Anneser et al., 2022), while chemogenetic activation of the Pth2-positive region of the rodent brain promotes social contact (Keller et al., 2022). Consistent with this, expression of *pth2* itself positively scales with the quantity of social interactions with conspecifics (Anneser et al., 2020; Anneser et al., 2022; Keller et al., 2022). In rodents, physical touch from conspecifics activates *Pth2* expression (Cservenák et al., 2013; Keller et al., 2022). In addition to tactile touch sensation, fish also have another form of “distant touch” through the mechanosensory lateral line (Dijkgraaf, 1963). The mechanosensory lateral line is a hair cell-based system in aquatic vertebrates that senses hydrodynamic information, such as that created by conspecifics (Groneberg et al., 2020; Montgomery et al., 2013). In zebrafish, chemical ablation of the mechanosensory lateral line prevents the rescue of *pth2* expression by a social environment following isolation (Anneser et al., 2020). Therefore, social “touch” (direct contact in rodents and hydrodynamic communication in zebrafish) seems to be a primary sensory activator of *pth2* expression.

Despite this knowledge, there remain several unanswered questions regarding the social regulation of *pth2* expression. First, how do zebrafish interpret social context when they are born without lateral line function? Secondly, do mechanosensory hair cells in the inner ear contribute to the ability of zebrafish larvae to respond to social context? Thirdly, is *pth2* expression regulated

solely via mechanosensation, or can fish use additional sensory inputs to sense the presence of conspecifics? Here, we report that the congenital loss of mechanosensory hair cell function leads to chronically depressed levels of *pth2* expression in socially-housed larval zebrafish. Interestingly, social isolation of hair cell mutants further decreases *pth2* levels, suggesting that larval fish use additional sensory information to sense conspecifics and modulate *pth2* expression. Lastly, we utilize fluorescent reporters driven by the *pth2* regulatory region to evaluate the morphology of *pth2*-expressing cells and visualize *pth2* dynamics *in vivo*. Overall, this study offers additional insight into the sensory basis for social interactions in zebrafish and introduces novel tools to track *pth2* expression in living fish.

RESULTS

Decreased *pth2* expression in larval zebrafish with a genetically disabled lateral line.

pth2 expression decreases when fish are raised in isolation but increases following a brief period of social interaction with conspecifics. However, when the mechanosensory lateral line is ablated in isolated fish prior to social exposure, *pth2* expression levels remain low (Anneser et al., 2020). This implicates the lateral line sensory system in recognizing conspecifics to stimulate *pth2* expression. To further evaluate the role of the lateral line in social recognition, we raised lateral line-deficient mutants (*lhfpl5b*$^{-/-}$) and their siblings in separate social groups and detected *pth2* expression by mRNA *in situ* hybridization (ISH). Socially-raised lateral line mutants exhibit a decrease in *pth2* expression compared to wild type (WT) siblings (Fig. 1B, C), both in terms of a qualitative decrease in the intensity of staining as well as a significant decrease in the number of detectable *pth2*-positive cells (One-tailed Welch's t-test, WT Soc: M = 29.9, SD = 1.7; MUT Soc: M = 9.7, SD = 4.3; $p < 0.0001$) (Fig. 1D). We also ablated lateral line hair cells in socially raised WT larvae using repeated neomycin treatments (Venuto and Erickson, 2021) (Figure 1E). Even though these larvae had social experience prior to losing lateral line input, they exhibited low levels of *pth2* expression similar to lateral line mutants. These results confirm that the loss of lateral line function impairs the ability of *pth2* cells to respond to social context.

Mechanosensory input from inner ear hair cells do not contribute to *pth2* expression.

A low level of *pth2* expression remains in socially-raised lateral line mutants (Fig. 1B, C). To determine if mechanosensory input from the inner ear was responsible for this remaining *pth2*

105 expression, we used three different types of mutations that disable hair cells of both the lateral line
106 and inner ear to compare to the lateral line mutant (*lhfpl5b*$^{-/-}$) and wild type zebrafish. Two of these
107 mutations (*pcdh15a*$^{-/-}$ and *tomt*$^{-/-}$) render the mechano-electrical transduction channel
108 nonfunctional in all hair cells, similar to how the *lhfpl5b* mutation specifically disables lateral line
109 hair cells (Erickson et al., 2017; Erickson et al., 2020; Maeda et al., 2017). The third mutant
110 disables the voltage-gated calcium channel in hair cells (*cacna1da*$^{-/-}$), thereby blocking stimulus-
111 dependent glutamate release (Sheets et al., 2012; Sidi et al., 2004). Again, we measured *pth2*
112 expression via mRNA ISH (Fig. 2B-F) as well as quantitative PCR (qPCR) (Fig. 2G). All hair cell
113 mutants exhibit similarly low levels of *pth2* expression when raised socially, with no additional
114 decrease seen in zebrafish with genetically disabled inner ear and lateral line sensory function
115 (One-way ANOVA with Tukey post-test, $\alpha = 0.05$). From these experiments, we find that inner
116 ear mechanosensory hair cells do not contribute to the regulation of *pth2* expression.
117
118 **Social isolation further reduces *pth2* expression in sensory hair cell mutants.**
119 Chemosensory and visual perception of conspecifics does not significantly rescue *pth2*
120 expression in larval zebrafish raised in isolation (Anneser, et al., 2020). However, since disabling
121 both the lateral line and the inner ear does not completely eliminate *pth2* expression, other non-
122 hair cell-based sensory systems may contribute to the modulation of *pth2* by social context. To test
123 this, we compared *pth2* expression in social and isolated *lhfpl5b* and *tomt* mutants by both mRNA
124 ISH (Fig. 3A-C) and qPCR (Fig. 3D). If *pth2* responds to conspecific signals solely via the lateral
125 line, we expect to see equivalently low expression in mutants raised in social and isolated
126 environments. However, we find this not to be the case. Instead, isolated *lhfpl5b* and *tomt* mutants
127 express less *pth2* than social mutant siblings (One-way ANOVA with Tukey post-test, $\alpha = 0.05$).
128 *pth2* levels in isolated mutants and wild types are indistinguishable. Because social isolation
129 further reduces *pth2* expression in lateral line mutants, we conclude that *pth2* responds to
130 multisensory input during social experience.
131
132 **Morphology of *pth2*-expressing cells using fluorescent reporters.**
133 Fluorescent reporters provide information about the morphology and function of cells,
134 along with the ability to quantify gene expression in living organisms (Choe et al., 2021; Soboleski
135 et al., 2005). Therefore, we created stable lines of transgenic zebrafish expressing GFP or RFP

136 under control of the presumptive *pth2* promoter. These transgenes allow us to visualize the
137 morphology of the *pth2*-expressing cells in living larvae (Fig. 4 and S1). Imaging of transgenic
138 larvae reveals the two bilateral cell clusters with complex projection patterns (Fig. 4B). The
139 anterior ipsilateral projections converge into a dense neuropil in the forebrain, while other fibers
140 project ventrally and posteriorly toward the midbrain. Additionally, we find ventral projections
141 that cross the midline between the two cell clusters. This morphology is consistent in both the GFP
142 and RFP transgenes.
143
144 **The *pth2* transgenes respond to lateral line input and social context.**
145 Next, we tested if the transgene responds to social context (Fig. 5). Consistent with our
146 mRNA ISH and qPCR results, transgenic *lhfpl5b* mutants (Fig. 5A-C) and isolates (Fig. 5D-F)
147 both exhibit a significant decrease in the number of fluorescent cells relative to control siblings
148 (Fig. 5C: One-tailed Welch's t-test, WT Soc: M = 43.2, SD = 3.9; MUT Soc: M = 34.2, SD = 2.8;
149 $p < 0.0001$) (Fig. 5F: One-tailed Welch's t-test, WT Soc: M = 37.3, SD = 2.6; WT Iso: M = 28.3,
150 SD = 2.8; $p < 0.0001$). To gauge whether isolation specifically diminishes expression from the
151 *pth2*-driven transgenes, we compared the effect of social isolation on transgene expression in
152 *Tg(pth2:TagRFP)unb3* and *Tg(slc6a3:EGFP)ot80* larvae. The *slc6a3:*EGFP transgene expresses
153 GFP under control of the *dopamine transporter* (*dat*) promoter and marks a population of
154 dopaminergic cells in the pretectum, which lies dorsally to the *pth2*-expressing cells. The number
155 of dopaminergic cells in the pretectum do not change in response to social context (One-tailed
156 Welch's t-test, WT Soc: M = 44.0, SD = 4.3; WT Iso: M = 45.1, SD = 4.7; $p = 0.3$) (Fig. 5D-F).
157 These experiments demonstrate that the *pth2* transgenes respond to social context and allows for
158 a wide variety of future experiments to better understand how *pth2* is regulated.
159
160 **DISCUSSION**
161 Previous work revealed that larval zebrafish use lateral line information to sense the
162 presence of conspecifics, leading to upregulation of the social hormone Pth2. Here, we show that
163 *pth2* levels are chronically depressed in socially-raised larvae born without lateral line function.
164 However, social isolation further reduces *pth2* levels in lateral line mutants, suggesting that other
165 socially-derived sensory information can modulate *pth2* expression.
166

167 **The mechanosensory lateral line mediates *pth2* expression.**

168 Anneser, et al. (2020) implicated hydrodynamic stimuli from conspecifics as a key social
169 cue that upregulates production of the neuropeptide Pth2. Isolated larvae with chemically ablated
170 lateral lines fail to upregulate *pth2* when returned to a social environment. In the present study, we
171 use mutant zebrafish with a congenital loss of lateral line function to confirm that hydrodynamic
172 information modulates *pth2* expression. Furthermore, we find that repeated chemical ablation of
173 the lateral line also impairs the ability of social larvae to express *pth2*, even when exposed to
174 conspecifics prior to loss of lateral line function. Our approach complements that of Anneser et al.
175 by providing genetic evidence that *pth2* is modulated by lateral line sensory information (Fig. 1).
176 We conclude that, in terms of Pth2 production, zebrafish born without a lateral line effectively feel
177 alone even when raised in a social context.

178

179 **Auditory and vestibular stimuli do not modulate *pth2* expression in larval zebrafish.**

180 Inner ear hair cells are functionally and structurally similar to lateral line hair cells, and
181 fish use auditory and vestibular sensory information in a variety of behaviors (Bagnall and
182 Schoppik, 2018; Kohashi et al., 2012; Nicolson et al., 1998; Privat et al., 2019). Given that some
183 *pth2* expression remains in lateral line mutants, we examined whether sensory information from
184 the inner ear contributes to social modulation of *pth2.* Using zebrafish with mutations that disable
185 both inner ear and the lateral line hair cells, we find that there is no additional loss of *pth2*
186 expression compared to the lateral line-only mutant (Fig. 2). In addition, we asked if different types
187 of mutations to hair cells impact *pth2* expression. Three of the mutant lines used in this study,
188 *lhfpl5b, tomt* and *pcdh15a,* render the mechanotransduction (MET) channel non-functional
189 (Erickson et al., 2017; Erickson et al., 2020; Maeda et al., 2017), and one mutant line, *cacna1da /*
190 *cav1.3a,* affects the voltage-gated calcium channel (Sheets et al., 2012; Sidi et al., 2004). While
191 both components are necessary for proper hair cell signal transduction, there are key differences
192 between the types of mutations. For mutants affecting the MET channel, potassium and calcium
193 ions are unable to enter the cell in response to stimuli, but the potential for spontaneous calcium
194 influx and neurotransmitter release remains (Trapani and Nicolson, 2011). Whereas for the
195 calcium channel mutation, ions enter through the MET channel but there is no evoked or
196 spontaneous neurotransmitter release. Regardless, all mutations that disrupt hair cell function
197 result in the same decrease of *pth2* expression in socially raised fish compared to their wild type

198 siblings (Fig. 2). Therefore, we conclude that regulation of *pth2* by social context is primarily via
199 the mechanosensory lateral line in larval zebrafish and that auditory and vestibular information
200 does not contribute.
201
202 **Additional socially-derived sensory cues modulate *pth2* expression.**
203 Anneser et al. (2020) demonstrated that neither chemical nor visual cues from conspecifics
204 significantly restored *pth2* expression in isolated larvae. In our study, we found that isolation
205 further reduced *pth2* expression in lateral line mutants to the same level as isolated wild types (Fig.
206 3). This indicates that additional sensory modalities contribute to the regulation of *pth2* expression.
207 It will be informative to test whether the photo- or chemosensory systems can modulate *pth2*
208 expression under sensitized circumstances in which hydrosensory information is compromised.
209 Additionally, it is possible that tactile stimuli are contributing to *pth2* regulation in zebrafish,
210 consistent with the effects of social touch in rodents. Future work is necessary to test this theory.
211
212 **Visualizing *pth2* expression *in vivo.***
213 We used *pth2* promoter-driven fluorescent transgenes to visualize *pth2*-expressing cells
214 and their projections. Consistent with the Anneser, et al. (2020) whole-mount immunostains, we
215 see Pth2-positive cells located in bilateral clusters in the thalamus that feature lateral neurites,
216 anterior ipsilateral projections terminating as a loosely organized neuropil in the telencephalon, as
217 well as posterior ipsilateral projections. The transgene reveals additional fibers that project
218 ventrally from the cell bodies and cross the midline, potentially contacting the contralateral *pth2*-
219 expressing cluster (Fig. 4 and Supplemental Movie 1). Investigating the morphology of these cells
220 will help us understand the cellular targets of Pth2 signaling and how activity of the two clusters
221 is coordinated.
222 We also tested the *pth2:EGFP* and *pth2:TagRFP* transgenic lines as a proxy for *pth2*
223 expression *in vivo* and found that both lateral line mutants and isolated wild type larvae exhibit
224 fewer GFP/RFP-positive cells than socially raised siblings (Fig. 5). In contrast, the number of
225 dopaminergic cells located dorsally to the *pth2* clusters exhibited no change to social context.
226 Dopamine has been implicated in sensation and social interaction (Haehnel-Taguchi et al., 2018;
227 Saif et al., 2013; Shams et al., 2018), and our results indicate that the social modulation of *pth2* is
228 distinct from the dopaminergic system in this brain region in larval zebrafish. While our results

229 with the *pth2* transgenes agree with our *in situ* hybridization and qPCR results (Fig. 1, 3), we note
230 that the effects of isolation and lateral line deficiency on transgene expression are not as
231 pronounced as when assaying for endogenous *pth2* mRNA and protein. It could be that the post-
232 transcriptional and / or post-translation regulation of fluorescent proteins do not reflect regulation
233 of endogenous *pth2* transcription and protein stability. It is also possible that the *pth2* promoter
234 region we use to drive the transgene is missing some critical regulatory elements. Future work will
235 strive to distinguish between these possibilities and to optimize the transgene for capturing *pth2*
236 properties in vivo.

237 Overall, our results confirm that *pth2* expression is modulated by the mechanosensory
238 lateral line (Fig. 1). We also show that the lateral line is the only hair-cell based sensory organ
239 regulating *pth2* expression (Fig. 2). However, due to expression levels being slightly higher in
240 social lateral line mutants compared to the same mutants or wild type larvae raised in isolation, we
241 conclude that there must be unidentified sensory system(s) that contribute to the modulation of
242 *pth2* (Fig. 3). Finally, we created transgenic lines to visualize the morphology of *pth2*+ cells *in*
243 *vivo* (Fig. 4), and report that the transgenes respond to social context (Fig. 5). These transgenic
244 lines can be used in future studies to elucidate the role of *pth2* in zebrafish. Taken together, this
245 work suggests that zebrafish without a functioning lateral line experience a chronic sense of
246 isolation, even in a social context.
247

248 **MATERIALS AND METHODS**

249 **Ethics statement**

250 Animal research complied with guidelines stipulated by the Institutional Animal Care and
251 Use Committees at East Carolina University (Greenville, NC, United States) and at University of
252 New Brunswick (Fredericton, New Brunswick, Canada). Zebrafish (*Danio rerio*) were maintained
253 and bred using standard procedures (Westerfield, 2000). All experiments used larvae at 1–5 days
254 post-fertilization (dpf), which are of indeterminate sex at this stage.
255

256 **Mutant and transgenic fish lines**

257 The following previously described zebrafish mutant and transgenic lines were used in this
258 study: *lhfpl5b*^{vo35}, *pcdh15a*^{th263b}, *tomt*^{tk256c}, *cacna1da*^{tc323d}, and *Tg(slc6a3:EGFP)ot80* (Erickson et
259 al., 2017; Erickson et al., 2020; Maeda et al., 2017; Sidi et al., 2004; Xi et al., 2011). To make the

260 *Tg(pth2:EGFP)unb2* and *Tg*(*pth2:TagRFP)unb3* transgenic lines, 2067 base pairs immediately
261 upstream of the *pth2* coding region (including the 5' UTR and first intron) were PCR amplified
262 with primers containing attB4-B1 recombination sites (*pth2*-specific sequence underlined: Fwd:
263 GGGGACAACTTTGTATAGAAAAGTTGGTAAAGGACACTCTTTGAGATCCT, Rvs:
264 GGGGACTGCTTTTTTGTACAAACTTGCCTGCAGATGAATAAGTTGAATAATACA. The
265 PCR product was cloned into the Gateway pDONR-P4-P1R entry vector by a standard BP clonase
266 reaction and an Multisite LR reaction was performed to create *pth2:EGFP-pA, cryaa:EGFP* and
267 *pth2:tagRFP-pA, cryaa:mCherry* plasmids. pDestTol2pACryGFP and pDESTtol2pACrymCherry
268 plasmids were gifts from Joachim Berger & Peter Currie (Addgene plasmids # 64022, 64023). The
269 expression constructs were co-injected with *tol2* transposase mRNA into 1-cell zebrafish embryos
270 (Kwan et al., 2007). F0 founders were outcrossed to produce stable F1 transgenics. At a minimum,
271 progeny from F2 transgenics were used in this study.
272
273 **Social isolation experiments for *in situ* hybridization, qPCR, and transgenic lines**
274 Zebrafish larvae were sorted for *lhfpl5b*^{vo35}, *pcdh15a*^{th263b}, *tomt*^{tk256c} homozygotes at 2 dpf
275 with FM1-43 dye labelling. *cacna1da*^{tc323d} homozygotes were identified behaviorally at 4 dpf.
276 *Tg*(*pth2:EGFP)* and *Tg*(*pth2:TagRFP)* transgenics were identified by their GFP or mCherry lens
277 markers, respectively. *Tg(slc6a3:EGFP)*-positive larvae were identified by GFP expression in the
278 brain. Identified larvae were divided into social groups of thirty larvae, while another thirty larvae
279 were placed in isolation. Both social and isolated larvae were housed in 6-well tissue culture plates
280 containing 5 ml of E3 embryo media. Strips of paper were placed between each well to prevent
281 visual access between wells. Larvae intended for mRNA *in situ* hybridization (ISH) were grown
282 in E3 with 200 µM N-Phenylthiourea (PTU) (Alfa Aesar) to prevent pigment formation. Each
283 group was incubated at 28.5ºC with a 14L:10D photoperiod from 2 to 4 dpf. At 4 dpf, larvae were
284 either fixed for *in situ* hybridization, processed for qPCR, or imaged to visualize the transgene.
285
286 **Repeated neomycin treatments**
287 The repeated neomycin treatments were performed essentially as previously described
288 (Venuto & Erickson, 2021). At 24 hpf, WT embryos were divided into two groups of 30 and
289 grown continuously in media supplemented with 200 µM PTU to prevent pigment formation.
290 Larvae were manually dechorionated at 2 dpf. Starting at 9:00 AM, 3 dpf larvae were exposed to

291 either 0 or 50 µM neomycin sulfate hydrate (Alfa Aesar) for 30 minutes at 28ºC every 12 hours.
292 At noon on 4 dpf, treated and untreated groups of larvae were anesthetized with 0.016% MS-222
293 and fixed in 4% PFA for mRNA ISH. The experiment was repeated twice using 30 larvae per
294 treatment group.
295
296 **mRNA in situ hybridization**
297 The *pth2* in situ probe sequence was amplified using the Invitrogen SuperScript IV One-
298 Step RT-PCR kit (ThermoFisher) using the following forward and reverse primers: F:
299 CATTGCATGGACGATTTACG; R: TGCCATGTCATTCAAAATCC. The RT-PCR product
300 was purified by gel extraction and propagated in the pCR4-TOPO vector. The pCR4-*pth2* plasmid
301 was linearized with NotI and the antisense DIG-labeled ISH probe was made using the T3 RNA
302 polymerase promoter. Probe synthesis and in situ hybridization were performed essentially as
303 described (Erickson et al., 2010). Larvae were imaged at 20X magnification using an Olympus
304 BH-2 microscope outfitted with a Jenoptik Gryphax Arktur camera.
305
306 **RNA isolation and real time quantitative PCR (qPCR)**
307 For RNA isolation, 10 whole larval heads were used per replicate. Samples were collected
308 on ice, placed in 1.7 mL RNase-free microcentrifuge tubes containing 200 µl RNAzol (Molecular
309 Research Center, Inc., OH. Catalog: RN 190) and homogenized immediately. Total RNA was
310 extracted from homogenized solutions according to the manufacturer's protocol. For each sample,
311 cDNAs was synthesized using 1 µg total RNA and a high-capacity cDNA Reverse Transcription
312 kit (Thermo Fisher Scientific, Waltham, Massachusetts, USA, Catalog#4368814) following the
313 manufacturer's instructions.
314 The levels of *pth2* transcripts were determined by quantitative real-time PCR (qPCR) using
315 SYBR green dye (Invitrogen) and a CFX Connect real-time thermal cycler (Bio-Rad Laboratories,
316 Hercules, California, USA). The qPCR reaction was conducted with initial denaturation at 95 °C
317 for 2 min, followed by 30 cycles of 30 s denaturation at 95 °C, 30 s annealing at 57 °C, and 30 s
318 extension at 72 °C using the specific primers (Forward: CCACGCAACACACAGTCAAG,
319 Reverse: GCAAGTTACTTTGCAGAGGTC) and GoTaq G2 DNA polymerase (Promega,
320 Madison, Wisconsin, USA). Each PCR mixture (15 µl) consisted of 7.795 µl DNase free water,
321 3 µl 5XGoTaq buffer, 1.5 µl 25 mM MgCl2, 0.3 µl 10 mM dNTP mix, 0.15 ml 10µM forward or

322 reverse primer, 2 µl cDNA, 0.03 µl 100X SYBR green dye (final concentration 0.2X), and 0.075
323 µl Taq. The absolute values (copies/µg total RNA) were determined using Ct values of samples
324 and a standard curve generated from serial known concentrations of plasmid containing the target
325 region of *pth2*. The relative expression was computed by calculating the fold change compared to
326 the mean value of the mutant isolated condition. The efficiency of the PCR and authentic PCR
327 products was further confirmed by analyses of melting curve and gel electrophoresis.
328
329 **Transgenic imaging and quantification**
330 Live zebrafish larvae were anesthetized with E3 plus 0.016% MS-222 and mounted
331 dorsally on a depression slide in 1.2% low melting point agarose in E3. EGFP was imaged using
332 a Zeiss LSM800 laser-scanning confocal with a 40x water objective and Zeiss Zen software. To
333 quantify results, cell counts were performed using Fiji/ImageJ image processing software
334 (Schindelin et al., 2012). Depth encoded 2D and 3D projections were created in Fiji/ImageJ using
335 the *Z-stack Depth Color Code 0.0.2* plugin. Figures were assembled in Adobe Photoshop and
336 equally adjusted for brightness and contrast among corresponding treatment groups.
337
338 **Statistical tests**
339 All graphs and statistical tests were done using R (R Core Team, 2021). For *in* situ
340 hybridization cell counts, a one-tailed Welch's t-test was used (two replicates, n = 7-9 larvae per
341 condition per replicate). For the qPCR experiment, a one-way ANOVA with a Tukey post-hoc test
342 was conducted (three replicates, n = 10 per condition per replicate). For the transgenic cell counts,
343 a one-tailed Welch's t-test was used (three replicates, n = 5 per condition per replicate). A p-value
344 of less than 0.05 was considered significant. One-way ANOVAs were used to compare the whole
345 experimental condition (genotype plus social context) as single independent variables. One-tailed
346 t-tests were used due to only having an expectation for a decrease in *pth2* expression following
347 isolation or loss of lateral line sensory information. Sample sizes were determined by the number
348 of fish used in the experiment. Replicates indicate how many times the experiment was conducted.
349 No samples were excluded from the analysis.
350
351
352

ACKNOWLEDGMENTS

The authors would like to thank Dr. Yong Zhu for providing his reagents and assistance with qPCR experiments, and Dr. Bryan Crawford for helpful comments on the manuscript. We also thank members of the Erickson and Issa labs for their assistance with zebrafish husbandry.

COMPETING INTERESTS

The authors declare no competing interests.

FUNDING

This work was funded by East Carolina University's Division of Research, Economic Development and Engagement (REDE) and The Natural Science and Engineering Research Council (NSERC) of Canada Discovery Grant RGPIN-2021-03166 to T.E.

DATA AVAILABILITY

The datasets generated for this study are available on request to the corresponding author.

REFERENCES

Amaral, D. G. (2002). The primate amygdala and the neurobiology of social behavior: implications for understanding social anxiety. *Biological Psychiatry* **51**, 11–17.

Anneser, L., Alcantara, I. C., Gemmer, A., Mirkes, K., Ryu, S. and Schuman, E. M. (2020). The neuropeptide Pth2 dynamically senses others via mechanosensation. *Nature 2020 588:7839* **588**, 653–657.

Anneser, L., Gemmer, A., Eilers, T., Alcantara, I. C., Loos, A.-Y., Ryu, S. and Schuman, E. M. (2022). The neuropeptide Pth2 modulates social behavior and anxiety in zebrafish. *iScience* **25**, 103868.

Bagnall, M. W. and Schoppik, D. (2018). Development of vestibular behaviors in zebrafish. *Curr Opin Neurobiol* **53**, 83.

Bhattacharya, P., Yan, Y. L., Postlethwait, J. and Rubin, D. A. (2011). Evolution of the vertebrate pth2 (TIP39) gene family and the regulation of PTH type 2 receptor (pth2r) and its endogenous ligand pth2 by hedgehog signaling in zebrafish development. *Journal of Endocrinology* **211**, 187–200.

384 **Brothers, L.** (1990). The neural basis of primate social communication. *Motivation and Emotion*
385 *1990 14:2* **14**, 81–91.
386 **Burgdorf, J. and Panksepp, J.** (2006). The neurobiology of positive emotions. *Neuroscience &*
387 *Biobehavioral Reviews* **30**, 173–187.
388 **Chen, P. and Hong, W.** (2018). Neural Circuit Mechanisms of Social Behavior. *Neuron* **98**, 16–
389 30.
390 **Choe, C. P., Choi, S.-Y., Kee, Y., Kim, M. J., Kim, S.-H., Lee, Y., Park, H.-C. and Ro, H.**
391 (2021). Transgenic fluorescent zebrafish lines that have revolutionized biomedical research.
392 *Laboratory Animal Research 2021 37:1* **37**, 1–29.
393 **Coutellier, L. and Usdin, T. B.** (2011). Enhanced long-term fear memory and increased anxiety
394 and depression-like behavior after exposure to an aversive event in mice lacking TIP39
395 signaling. *Behavioural Brain Research* **222**, 265–269.
396 **Cservenák, M., Szabó, É. R., Bodnár, I., Lékó, A., Palkovits, M., Nagy, G. M., Usdin, T. B.**
397 **and Dobolyi, A.** (2013). Thalamic neuropeptide mediating the effects of nursing on
398 lactation and maternal motivation. *Psychoneuroendocrinology* **38**, 3070–3084.
399 **Dijkgraaf, S.** (1963). The functioning and significance of the lateral-line organs. *Biological*
400 *Reviews* **38**, 51–105.
401 **Dimitrov, E. and Usdin, T. B.** (2010). Tuberoinfundibular peptide of 39 residues modulates the
402 mouse hypothalamic-pituitary-adrenal axis via paraventricular glutamatergic neurons. *J*
403 *Comp Neurol* **518**, 4375–4394.
404 **Dimitrov, E. L., Petrus, E. and Usdin, T. B.** (2010). Tuberoinfundibular peptide of 39 residues
405 (TIP39) signaling modulates acute and tonic nociception. *Experimental Neurology* **226**, 68–
406 83.
407 **Dimitrov, E. L., Kuo, J., Kohno, K. and Usdin, T. B.** (2013). Neuropathic and inflammatory
408 pain are modulated by tuberoinfundibular peptide of 39 residues. *Proceedings of the*
409 *National Academy of Sciences* **110**, 13156–13161.
410 **Dobolyi, A., Dimitrov, E., Palkovits, M. and Usdin, T. B.** (2012). The Neuroendocrine
411 Functions of the Parathyroid Hormone 2 Receptor. *Frontiers in Endocrinology* **3**, 121.
412 **Erickson, T., French, C. R. and Waskiewicz, A. J.** (2010). Meis1 specifies positional
413 information in the retina and tectum to organize the zebrafish visual system. *Neural*
414 *Development* **5**, 22.

415 **Erickson, T., Morgan, C. P., Olt, J., Hardy, K., Busch-Nentwich, E., Maeda, R., Clemens,**
416 **R., Krey, J. F., Nechiporuk, A., Barr-Gillespie, P. G., et al.** (2017). Integration of
417 Tmc1/2 into the mechanotransduction complex in zebrafish hair cells is regulated by
418 Transmembrane O-methyltransferase (Tomt). *Elife* **6**,.
419 **Erickson, T., Pacentine, I. v., Venuto, A., Clemens, R. and Nicolson, T.** (2020). The lhfpl5
420 Ohnologs lhfpl5a and lhfpl5b Are Required for Mechanotransduction in Distinct
421 Populations of Sensory Hair Cells in Zebrafish. *Frontiers in Molecular Neuroscience* **12**,
422 320.
423 **Groneberg, A. H., Marques, J. C., Martins, A. L., Diez del Corral, R., de Polavieja, G. G.**
424 **and Orger, M. B.** (2020). Early-Life Social Experience Shapes Social Avoidance
425 Reactions in Larval Zebrafish. *Current Biology* **30**, 4009-4021.e4.
426 **Haehnel-Taguchi, M., Fernandes, A. M., Böhler, M., Schmitt, I., Tittel, L. and Driever, W.**
427 (2018). Projections of the diencephalospinal dopaminergic system to peripheral sense
428 organs in larval zebrafish (Danio rerio). *Frontiers in Neuroanatomy* **12**, 20.
429 **Keller, D., Láng, T., Cservenák, M., Puska, G., Barna, J., Csillag, V., Farkas, I., Zelena, D.,**
430 **Dóra, F., Barteczko, L., et al.** (2022). A thalamo-preoptic pathway promoting social touch.
431 *bioRxiv* 2022.01.11.475648.
432 **Kohashi, T., Nakata, N. and Oda, Y.** (2012). Effective Sensory Modality Activating an Escape
433 Triggering Neuron Switches during Early Development in Zebrafish. *The Journal of*
434 *Neuroscience* **32**, 5810.
435 **Kolb, B. and Whishaw, I. Q.** (2003). Brain Plasticity and Behavior.
436 *http://dx.doi.org/10.1146/annurev.psych.49.1.43* **49**, 43–64.
437 **Kravitz, E. A. and Huber, R.** (2003). Aggression in invertebrates. *Current Opinion in*
438 *Neurobiology* **13**, 736–743.
439 **Kwan, K. M., Fujimoto, E., Grabher, C., Mangum, B. D., Hardy, M. E., Campbell, D. S.,**
440 **Parant, J. M., Yost, H. J., Kanki, J. P. and Chien, C.-B.** (2007). The Tol2kit: a multisite
441 gateway-based construction kit for Tol2 transposon transgenesis constructs. *Dev Dyn* **236**,
442 3088–99.
443 **LaBuda, C. J. and Usdin, T. B.** (2004). Tuberoinfundibular peptide of 39 residues decreases
444 pain-related affective behavior. *NeuroReport* **15**, 1779–1782.

445 **LaBuda, C. J., Dobolyi, A. and Usdin, T. B.** (2004). Tuberoinfundibular peptide of 39 residues
446 produces anxiolytic and antidepressant actions. *Neuroreport* **15**, 881–885.
447 **Maeda, R., Pacentine, I. v., Erickson, T. and Nicolson, T.** (2017). Functional Analysis of the
448 Transmembrane and Cytoplasmic Domains of Pcdh15a in Zebrafish Hair Cells. *The Journal*
449 *of Neuroscience* **37**, 3231–3245.
450 **Montgomery, J., Bleckmann, H. and Coombs, S.** (2013). Sensory Ecology and Neuroethology
451 of the Lateral Line. 121–150.
452 **Mumtaz, F., Khan, M. I., Zubair, M. and Dehpour, A. R.** (2018). Neurobiology and
453 consequences of social isolation stress in animal model—A comprehensive review.
454 *Biomedicine & Pharmacotherapy* **105**, 1205–1222.
455 **Neumann, I. D., Veenema, A. H. and Beiderbeck, D. I.** (2010). Aggression and anxiety: Social
456 context and neurobiological links. *Frontiers in Behavioral Neuroscience* **4**, 12.
457 **Nicolson, T., Rüsch, A., Friedrich, R. W., Granato, M., Ruppersberg, J. P. and Nüsslein-**
458 **Volhard, C.** (1998). Genetic Analysis of Vertebrate Sensory Hair Cell Mechanosensation:
459 the Zebrafish Circler Mutants. *Neuron* **20**, 271–283.
460 **Oldfield, R. G. and Hofmann, H. A.** (2011). Neuropeptide regulation of social behavior in a
461 monogamous cichlid fish. *Physiology & Behavior* **102**, 296–303.
462 **Panksepp, J. and Burgdorf, J.** (2003). "Laughing" rats and the evolutionary antecedents of
463 human joy? *Physiology & Behavior* **79**, 533–547.
464 **Panksepp, J., Burgdorf, J., Beinfeld, M. C., Kroes, R. A. and Moskal, J. R.** (2007). Brain
465 Regional Neuropeptide Changes Resulting From Social Defeat. *Behavioral Neuroscience*
466 **121**, 1364–1371.
467 **Privat, M., Romano, S. A., Pietri, T., Jouary, A., Boulanger-Weill, J., Elbaz, N., Duchemin,**
468 **A., Soares, D. and Sumbre, G.** (2019). Sensorimotor Transformations in the Zebrafish
469 Auditory System. *Current Biology* **29**, 4010-4023.e4.
470 **R Core Team** (2021). R: A Language and Environment for Statistical Computing.
471 **Robinson, G. E., Fernald, R. D. and Clayton, D. F.** (2008). Genes and social behavior. *Science*
472 **322**, 896–900.
473 **Saif, M., Chatterjee, D., Buske, C. and Gerlai, R.** (2013). Sight of conspecific images induces
474 changes in neurochemistry in zebrafish. *Behavioural Brain Research* **243**, 294–299.

475 **Schindelin, J., Arganda-Carreras, I., Frise, E., Kaynig, V., Longair, M., Pietzsch, T.,**
476 **Preibisch, S., Rueden, C., Saalfeld, S., Schmid, B., et al.** (2012). Fiji: an open-source
477 platform for biological-image analysis. *Nature Methods 2012 9:7* **9**, 676–682.
478 **Seitz, N.** (2019). Characterization Of Pth Type-2 Receptor (pth2rb) And Its Endogenous Ligand
479 Pth2 In Zebrafish Development. *Theses and Dissertations*.
480 **Shams, S., Seguin, D., Facciol, A., Chatterjee, D. and Gerlai, R.** (2017). Effect of social
481 isolation on anxiety-related behaviors, cortisol, and monoamines in adult zebrafish.
482 *Behavioral Neuroscience* **131**, 492–504.
483 **Shams, S., Amlani, S., Buske, C., Chatterjee, D. and Gerlai, R.** (2018). Developmental social
484 isolation affects adult behavior, social interaction, and dopamine metabolite levels in
485 zebrafish. *Developmental Psychobiology* **60**, 43–56.
486 **Sheets, L., Kindt, K. S. and Nicolson, T.** (2012). Presynaptic CaV1.3 Channels Regulate
487 Synaptic Ribbon Size and Are Required for Synaptic Maintenance in Sensory Hair Cells.
488 *The Journal of Neuroscience* **32**, 17273.
489 **Sidi, S., Busch-Nentwich, E., Friedrich, R., Schoenberger, U. and Nicolson, T.** (2004).
490 gemini Encodes a Zebrafish L-Type Calcium Channel That Localizes at Sensory Hair Cell
491 Ribbon Synapses. *The Journal of Neuroscience* **24**, 4213.
492 **Soboleski, M. R., Oaks, J. and Halford, W. P.** (2005). Green fluorescent protein is a
493 quantitative reporter of gene expression in individual eukaryotic cells. *The FASEB journal :*
494 *official publication of the Federation of American Societies for Experimental Biology* **19**,
495 440.
496 **Trapani, J. G. and Nicolson, T.** (2011). Mechanism of Spontaneous Activity in Afferent
497 Neurons of the Zebrafish Lateral-Line Organ. *The Journal of Neuroscience* **31**, 1614.
498 **Venuto, A. and Erickson, T.** (2021). Evaluating the Death and Recovery of Lateral Line Hair
499 Cells Following Repeated Neomycin Treatments. *Life* **11**, 1180.
500 **Weiss, I. C., Pryce, C. R., Jongen-Rêlo, A. L., Nanz-Bahr, N. I. and Feldon, J.** (2004). Effect
501 of social isolation on stress-related behavioural and neuroendocrine state in the rat.
502 *Behavioural Brain Research* **152**, 279–295.
503 **Wu, Q., Wen, T., Lee, G., Park, J. H., Cai, H. N. and Shen, P.** (2003). Developmental Control
504 of Foraging and Social Behavior by the Drosophila Neuropeptide Y-like System. *Neuron*
505 **39**, 147–161.

506 **Xi, Y., Yu, M., Godoy, R., Hatch, G., Poitras, L. and Ekker, M.** (2011). Transgenic zebrafish
507 expressing green fluorescent protein in dopaminergic neurons of the ventral diencephalon.
508 *Developmental Dynamics* **240**, 2539–2547.
509
510

511 **FIGURES AND LEGENDS:**

512

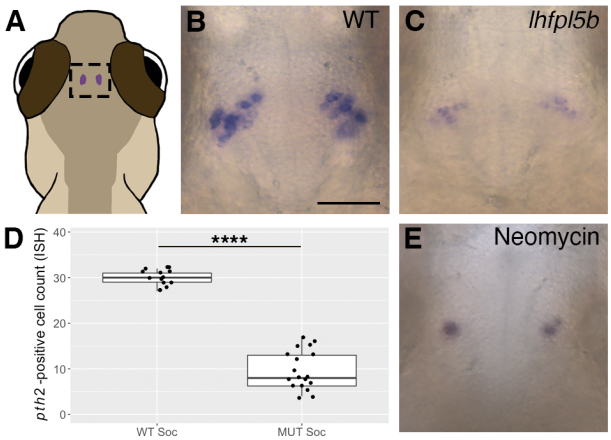

513

514 **Figure 1: Decreased *pth2* expression in lateral line-deficient larval zebrafish.** A: Location of
515 *pth2*-expressing cells in the thalamus. B-C: Representative images of mRNA *in situ* hybridizations
516 (ISH) showing *pth2*-positive cells in socially-reared B) wild type and C) lateral line mutant
517 (*lhfpl5b*^{vo35}) zebrafish at 4 dpf. D) Boxplots of *pth2*-positive cell counts from ISH images (WT =
518 14, MUT = 18 larvae from two replicates). E) Representative mRNA ISH image showing reduced
519 *pth2* expression in a socially-reared larva at 4 dpf whose lateral line was ablated with repeated
520 neomycin treatments. Scale bar is 50 µm and applies to all images. A one-tailed Welch's t-test was
521 used to assess significance, **** = $p < 0.0001$.

522

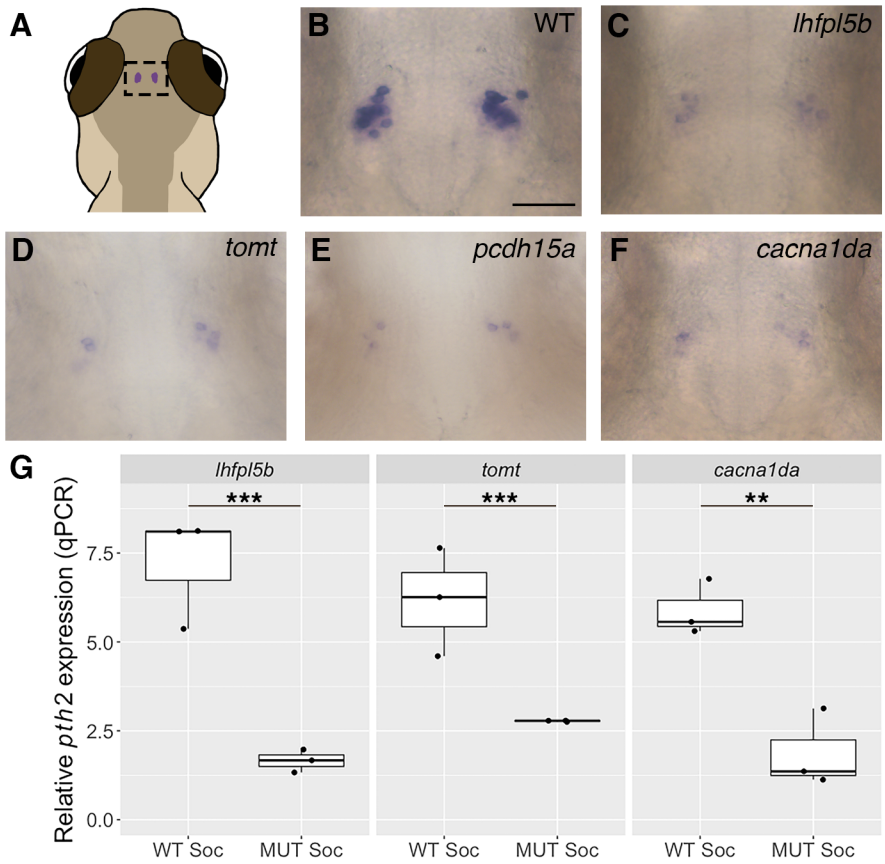

Figure 2: Mechanosensory input from inner ear hair cells does not contribute to *pth2* expression. A: Location of *pth2*-expressing cells in the thalamus. B-F: Representative images of mRNA *in situ* hybridizations (ISH) showing *pth2*-positive cells in socially-reared B) wild type, C) *lhfpl5b*^{vo35}, D) *tomt*^{tk256c}, E) *pcdh15a*^{th263b}, and F) *cacna1da*^{tc323d} larvae at 4 dpf. Scale bar = 50 µm, applies to all images. G: Boxplots of qPCR results showing *pth2* expression in socially-reared mutants and siblings. Three replicates per condition, n = 10 larvae per condition per replicate. One way ANOVA with Tukey post-test to assess significance, *** = $p < 0.001$, ** = $p < 0.01$.

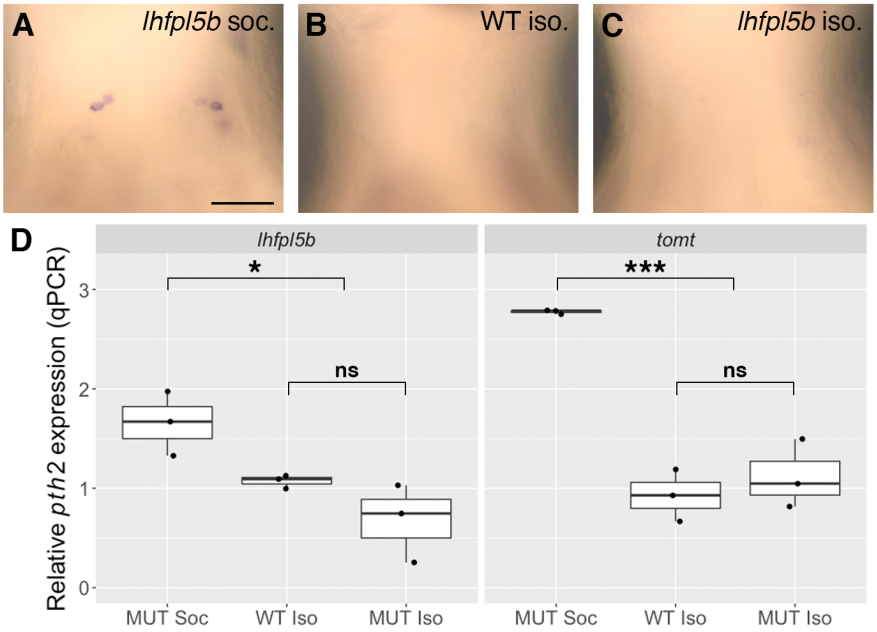

Figure 3: Social isolation further reduces *pth2* expression in sensory hair cell mutants. A-C: mRNA *in situ* hybridization showing representative examples of *pth2*-positive cells in A) socially-reared *lhfpl5b*^{vo35} mutants, B) isolated wild type larvae, and C) isolated *lhfpl5b*^{vo35} mutants. Scale bar = 50 µm, applies to all images. D: Boxplots of qPCR results comparing *pth2* expression in socially-reared *lhfpl5b*^{vo35} and *tomt*^{tk256c} mutants relative to isolated mutant and wild type siblings. Three replicates per condition, n = 10 larvae per condition per replicate. One way ANOVA with Tukey post-test to assess significance, *** = $p < 0.001$, * = $p < 0.05$, ns = not significant.

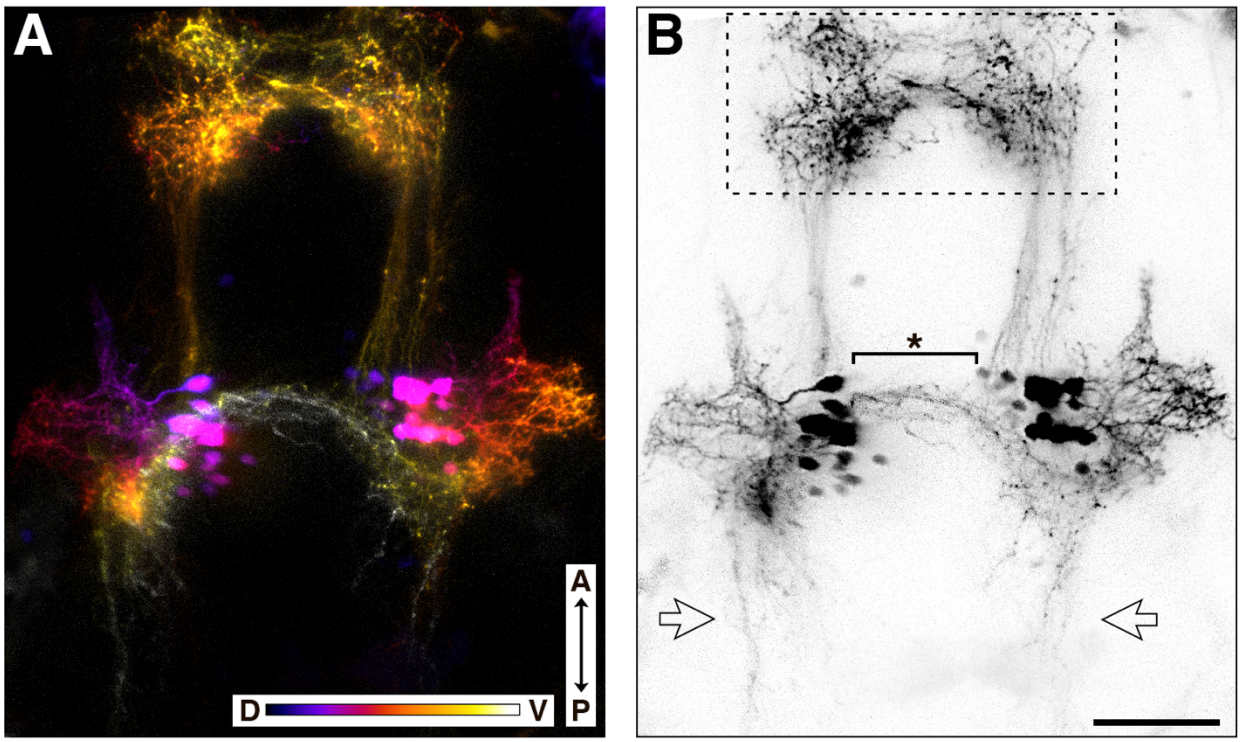

Figure 4: Morphology of *pth2*-expressing cells. A: Representative depth-encoded image of the *Tg(pth2:TagRFP)unb3* transgenic line at 4 dpf. The anterior-posterior (A-P) axis and dorsal-ventral (D-V) depth color scale are indicated at the bottom. B: Black and white version of the image in A. From the top: the dashed box indicates the anterior neuropil, the starred bracket highlights the ventral neurites that cross the midline, and the bilateral open arrows point to posterior neurites. Scale bar in B is 50 µm, applies to both images. See Supplemental Movie 1 for a 3D rendering of the depth-encoded *pth2* transgene.

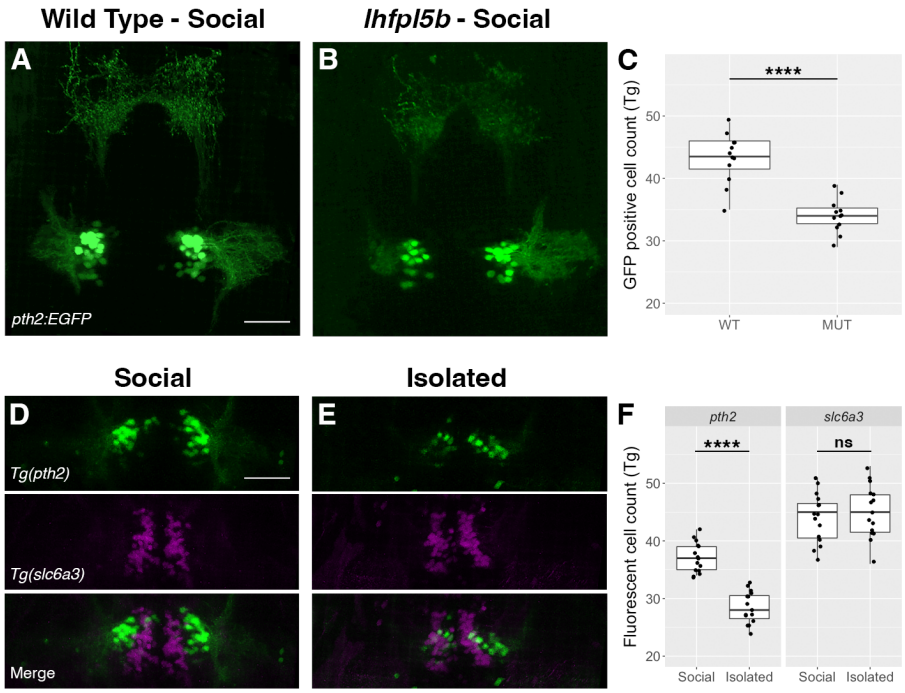

Figure 5: Effect of lateral line loss of function and social isolation on *pth2* and *slc6a3* expression using fluorescent reporters. A-B: Representative images of *Tg*(*pth2:EGFP)unb2* transgenic expression in socially-reared A) wild type and B) lateral line mutant (*lhfpl5b*^{vo35}) zebrafish. C) Boxplots of GFP-positive cell counts in wild type (WT) and *lhfpl5b* mutant (MUT) siblings. D-E: Representative images of *Tg*(*pth2:TagRFP)unb3* (false-colored green, top) and *Tg(slc6a3:EGFP)ot80* (false-colored magenta, middle) transgenes in D) socially-reared and E) isolated larvae. Merges of the two channels are shown at the bottom. F) Boxplots of *pth2* and *slc6a3* cell counts. Scale bar is 50 µm. A one-tailed Welch's t-test was used to assess significance, **** = $p < 0.0001$, ns = not significant.